ASYMPTOTIC THEORY OF SEPARATION AND REATTACHMENT OF A LAMINAR BOUNDARY LAYER ON A COMPRESSION RAMP

O. R. Burggraf

Ohio State University Research Foundation

Prepared for:

Office of Naval Research

May 1975

RF Project 3303
Technical Report 3

the ohio state university
research foundation
1314 kinnear road
columbus, ohio
43212

ASYMPTOTIC THEORY OF SEPARATION AND REATTACHMENT OF A LAMINAR BOUNDARY LAYER ON A COMPRESSION RAMP

O.R. Burggraf

Department of Aeronautical and Astronautical Engineering

Office of Naval Research
Fluid Dynamics Program
Arlington, Virginia 22217

Contract N00014-67-A-0232-0014
NR 061-194

May 1975

Presented at the Symposium on "Flow Separation" sponsored by the AGARD Fluid Dynamics Panel, May 27-30, 1975, Göttingen, Germany

Unclassified

SECURITY CLASSIFICATION OF THIS PAGE (When Data Entered)

REPORT DOCUMENTATION PAGE		READ INSTRUCTIONS BEFORE COMPLETING FORM
1. REPORT NUMBER	2. GOVT ACCESSION NO.	3. RECIPIENT'S CATALOG NUMBER
4. TITLE (and Subtitle) ASYMPTOTIC THEORY OF SEPARATION AND REATTACHMENT OF A LAMINAR BOUNDARY LAYER ON A COMPRESSION RAMP		5. TYPE OF REPORT & PERIOD COVERED Technical Preprint 6. PERFORMING ORG. REPORT NUMBER
7. AUTHOR(s) O.R. Burggraf		8. CONTRACT OR GRANT NUMBER(s) N00014-67-A-0232-0014
9. PERFORMING ORGANIZATION NAME AND ADDRESS The Ohio State University Research Foundation 1314 Kinnear Road, Columbus, Ohio 43212		10. PROGRAM ELEMENT, PROJECT, TASK AREA & WORK UNIT NUMBERS NR 061-194
11. CONTROLLING OFFICE NAME AND ADDRESS Department of the Navy Office of Naval Research Arlington, Virginia 22217		12. REPORT DATE May 1975 13. NUMBER OF PAGES 12,
14. MONITORING AGENCY NAME & ADDRESS(if different from Controlling Office)		15. SECURITY CLASS. (of this report) Unclassified 15a. DECLASSIFICATION/DOWNGRADING SCHEDULE

16. DISTRIBUTION STATEMENT (of this Report)

Reproduction in whole or in part is permitted for any purpose of the United States Government.

17. DISTRIBUTION STATEMENT (of the abstract entered in Block 20, if different from Report)

18. SUPPLEMENTARY NOTES

19. KEY WORDS (Continue on reverse side if necessary and identify by block number)

Boundary Layer; Separated Flow; Supersonic Flow; Compression Ramp

20. ABSTRACT (Continue on reverse side if necessary and identify by block number)

Laminar boundary layer separation and reattachment is here considered for adiabatic flow over a compression ramp with supersonic mainstream. For large ramp angle, calculations based on the Stewartson-Williams "triple-deck" theory show that the regions of separation and reattachment become distinct, with an intervening (plateau) region of nearly constant pressure. The mathematical description of each of these distinct regions is giv[illegible],

DD FORM 1 JAN 73 1473 EDITION OF 1 NOV 65 IS OBSOLETE

PRICES SUBJECT TO CHANGE

Unclassified

SECURITY CLASSIFICATION OF THIS PAGE (When Data Entered)

20.
and simple formulas derived for a number of quantities of interest, including the plateau pressure, conditions at separation and reattachment, and the geometry of the separated region. Detailed comparisons of the theoretical results with available experimental data show favorable agreement, suggesting that the theory can provide a useful tool for engineering analysis.

ASYMPTOTIC THEORY OF SEPARATION AND REATTACHMENT OF A LAMINAR BOUNDARY LAYER ON A COMPRESSION RAMP*

by
Odus R. Burggraf
Dept. of Aeronautical Engineering
The Ohio State University
2036 Neil Ave.
Columbus, Ohio 43210

SUMMARY

Laminar boundary layer separation and reattachment is here considered for adiabatic flow over a compression ramp with supersonic mainstream. For large ramp angle, calculations based on the Stewartson-Williams "triple-deck" theory show that the regions of separation and reattachment become distinct, with an intervening (plateau) region of nearly constant pressure. The mathematical description of each of these distinct regions is given, and simple formulas derived for a number of quantities of interest, including the plateau pressure, conditions at separation and reattachment, and the geometry of the separated region. Detailed comparisons of the theoretical results with available experimental data show favorable agreement, suggesting that the theory can provide a useful tool for engineering analysis.

1. INTRODUCTION

The boundary-layer concept has often been useful as a basis for calculating separated flows in supersonic main streams. When combined with a viscous interaction condition coupling the pressure to the displacement thickness, the boundary-layer equations appear to be an accurate model for certain types of separated flows at moderate Reynolds numbers of practical interest. Examples of the success of these methods are given by the work of Lees and Reeves[1] and of Nielsen.[2] At high Reynolds number R, the boundary layer with viscous interaction has been shown to develop a substructure,[3-5] which Stewartson has named the triple-deck. Computations have been carried out on the basis of triple-deck theory by Jenson, Burggraf and Rizzetta,[6] for the case of a compression ramp with supersonic mainstream. These results show that separation first occurs when the ramp angle α is of order $R^{-1/4}$. As α increases above those values reported in Ref. 6 (but still of order $R^{-1/4}$), a prominent pressure plateau develops between the distinct regions of separation and reattachment (see Fig. 1). Each of these regions has a distinct mathematical description for α large and relatively simple formulas have been derived for a number of quantities of interest. The purpose of this paper is to describe the mathematical structure of the separation, plateau, and reattachment regions and to compare the theoretical results with available experimental data, as outlined below.

2. SEPARATION AND PLATEAU REGIONS

The mathematical structure of the separation region has been given by Stewartson and Williams.[5] Briefly, the boundary layer is disturbed by some downstream obstacle, in this case a ramp. For large enough disturbance, the boundary layer will separate in a distance of order $R^{-3/8}$ ahead of the obstacle. Because of the short streamwise distance, viscous effects are restricted to a sublayer with thickness of order $R^{-5/8}$, while the main portion of the flow in the boundary layer continues as an inviscid rotational flow on the $R^{-3/8}$ length scale. Outside the boundary layer, the pressure disturbance is felt over a distance of order $R^{-3/8}$ in both transverse and longitudinal directions. If the separation point is far enough in front of the obstacle, as for the ramp of Fig. 1, the pressure asymptotes the plateau pressure downstream. This constant pressure region corresponds to an equivalent wedge surface running from separation point S to reattachment point R (see Fig. 2).

The asymptotic structure of the flow leaving the separation region has been described by Neiland[4] as a separated shear layer (centered on the equivalent wedge surface), an inviscid reversed flow which feeds the fluid entrained by the shear layer, and a reversed-flow boundary layer. The latter two flows decay with increasing x and are of no further concern to us. However, the velocity in the free shear layer grows with x.

For definiteness, let x, y, u, v, p, α be the physical coordinates, velocity, pressure, and ramp angle, and let X, Z, U, V, P, $\bar{\alpha}$ be the corresponding nondimensional quantities in the sublayer. Following Stewartson and Williams,[5] these are related as

$$\begin{aligned} x &= x_0 + \epsilon^3 a X \quad , \quad y = \epsilon^5 b Z \\ p &= p_0 + \epsilon^2 c P(X) \quad , \quad \alpha = \epsilon^2 (b/a)\bar{\alpha} \\ u &= \epsilon (d/b) U(X,Z) \quad , \quad v = \epsilon^3 (d/a) V(X,Z) \end{aligned} \tag{1}$$

Here $\epsilon = R_*^{-1/8}$, where R is the Reynolds number, and the asterisk subscript refers to a convenient reference state of the external flow in the interaction region. x_0 is a convenient reference length measured to some point in the interaction region, and p_0 is the pressure at the beginning of interaction. The parameters are defined as

$$\begin{aligned} a &= x_0 C^{3/8} \lambda^{-3/4} (M_*^2 - 1)^{-3/8} (T_w/T_\infty)^{3/2} \\ b &= x_0 C^{5/8} \lambda^{-3/4} (M_*^2 - 1)^{-1/8} (T_w/T_\infty)^{3/2} \\ c &= \rho_\infty u_\infty^2 C^{1/4} \lambda^{1/2} (M_*^2 - 1)^{-1/4} \\ d &= x_0 u_\infty C^{3/4} \lambda^{-1/2} (M_*^2 - 1)^{-1/4} (T_w/T_\infty)^2 \end{aligned} \tag{2}$$

*The research reported here was sponsored by the Office of Naval Research, United States Navy, under Contract No. N00014-07-A-0232-0014

λ takes the familiar value 0.332 when the undisturbed boundary layer is of the compressible Blasius type. C is the Chapman-Rubesin constant and the other variables have their usual meaning.

The flow in the sublayer is governed to first order by the classical incompressible boundary layer equations

$$U_X + V_Z = 0 \tag{4a}$$

$$UU_X + VU_Z = -P_X + U_{ZZ} \tag{4b}$$

subject to the usual no-slip condition on the wall streamline. However, the outer boundary condition is unconventional; it is an expression of the viscous interaction condition obtained by matching to the disturbed main boundary-layer flow, as described by Stewartson and Williams:[5]

$$P(X) = -A'(X) \quad , \quad A(X) = \lim_{Z \to \infty} (U-Z) \tag{5}$$

and A(X) approaches zero as $X \to -\infty$.

Jenson, Burggraf, and Rizzetta[6] have presented numerical solutions of the inner layer problem for the compression ramp, showing that separation first occurs for $\bar{\alpha} \approx 1.6$. The first indications of a pressure plateau appear for $\bar{\alpha} \approx 2.5$, and a fully developed plateau exists for $\bar{\alpha} = 3.5$ as shown by Fig. 1. The length of the plateau grows rapidly with increasing $\bar{\alpha}$, and for large $\bar{\alpha}$ the separation region appears to be pushed far ahead of the corner (on the $R^{-3/8}$ interaction scale). Hence the asymptotic structure described by Neiland is appropriate to the plateau shear layer when $\bar{\alpha}$ is large.

The shear layer leaving the separation region is described by Neiland,[4] and more fully by Stewartson and Williams,[7] in the form of asymptotic series:

$$U = X^{1/3} f_0'(\eta) + X^{-1/3} f_2'(\eta) + \cdots \tag{6a}$$

$$P = P_0 + P_2 X^{-2/3} + \cdots \tag{6b}$$

where

$$\eta = [Z - A(X)]/X^{1/3} \tag{6c}$$

The functions f_0 and f_2 satisfy the usual type of third-order ordinary differential equation. It suffices here to note that

$$f_0' = 0.9341 \quad , \quad f_2' = -0.2711 \quad \text{when} \quad f_0 = f_2 = 0. \tag{7}$$

The plateau pressure P_0 has been evaluated by Williams[7] by numerically solving the full inner-layer equations of the triple-deck, requiring that the reversed flow downstream of separation have the asymptotic form given by Neiland. P_0 was found to have the value 1.800, which is seen to agree very well with the plateau pressure of Fig. 1. This suggests that 3.5 is a sufficiently large value of $\bar{\alpha}$ for the asymptotic theory to apply.

Figure 3 is a comparison of the separation-region pressure predicted by the triple-deck theory with experimental data of Chapman, Kuehn and Larsen[8] for a forward-facing step. The reference state has been taken as conditions at the separation point (X = 0). The theory is seen to anticipate the initial pressure rise, but the agreement is quite good following separation. Another case is shown in Figure 4, corresponding to a curved ramp whose foot is tangent to the upstream plate. Two choices of reference state are shown here: (1) the solid symbols are for M_* equal initial freestream conditions, R_* equal to separation conditions, as was chosen in Ref. 5: (2) the open circles are for M_*, R_* both equal to separation point conditions. The latter choice makes the agreement better, although not of the quality of Fig. 3. This dependence on reference state is an effect of finite Reynolds number since the distance between the points is of order $R^{-3/8}$ and the pressure rise of order $R^{-1/4}$ according to the theory.

3. REATTACHMENT REGION

The flow in this region is fed by the separated shear layer, which is described by Neiland's asymptotic expression given above. Hence it is possible to estimate the orders of magnitude of the various terms in the Navier-Stokes equations for the reattachment region from the shear-layer scaling.

From Eqs. (6) and (1), the flow in the shear layer entering the reattachment region scales as follows:

$$u \sim L_p^{1/3} \quad , \quad y \sim L_p^{1/3} R^{-1/2}$$

where L_p is the length of the pressure plateau. Thus the inertia terms in the equations of motion scale as

$$u \frac{\partial u}{\partial x} \sim L_p^{2/3}/L_R$$

where L_R is the length scale of the reattachment region. The viscous term scales as

$$R^{-1} \frac{\partial^2 u}{\partial y^2} \sim L_p^{-1/3}$$

and from linear theory for supersonic flow $\Delta p \sim \alpha$ so that the pressure term scales as

$$\frac{\partial p}{\partial x} \sim \alpha / L_R$$

From continuity,

$$v \sim L_p^{2/3}/(L_R R^{1/2})$$

and requiring $v \sim \alpha u$ yields

$$L_R \sim L_p^{1/3}/(\alpha R^{1/2})$$

We now make the assumption that for large $\bar{\alpha}$ the pressure rise in reattachment is of the order of the dynamic pressure of the flow entering the reattachment region; i.e.

$$u^2 \sim \alpha$$

Hence

$$\begin{aligned} L_p &\sim \alpha^{3/2} \\ L_R &\sim \alpha^{-1/2} R^{-1/2} \end{aligned} \tag{8}$$

Summarizing, we find in the x-momentum equation

$$\text{Inertia Terms:} \quad u \frac{\partial u}{\partial x} \sim \alpha^{3/2} R^{1/2} \tag{9a}$$

$$\text{Viscous Term:} \quad \frac{1}{R} \frac{\partial^2 u}{\partial y^2} \sim \alpha^{-1/2} \tag{9b}$$

$$\text{Pressure Gradient:} \quad \frac{\partial p}{\partial x} \sim \alpha^{3/2} R^{1/2} \tag{9c}$$

A similar treatment of the y-momentum equation yields

$$\text{Inertia Terms:} \quad u \frac{\partial v}{\partial x} \sim \alpha^{3/2} R^{1/2} \tag{9d}$$

$$\text{Viscous Term:} \quad R^{-1} \frac{\partial^2 v}{\partial y^2} \sim \alpha^{1/2} \tag{9e}$$

$$\text{Pressure Gradient:} \quad \frac{\partial p}{\partial y} \sim \alpha^{1/2} R^{1/2} \tag{9f}$$

For $\alpha \sim R^{-1/4}$ ($\bar{\alpha} \sim 1$) as in the inner layer scaling of Eq. (1), all three terms in the x-momentum equation are of the same order, while the y-momentum equation reduces to

$$\frac{\partial p}{\partial y} = 0 \tag{10}$$

so that the conventional boundary-layer equations apply, as in Eq. (4). This scaling corresponds to $\bar{\alpha}$ less than about 3 (according to Ref. 6) where separation and reattachment both take place on the same length scale and the pressure plateau has not fully developed.

Alternatively if we require $\alpha \sim R^{-1/4}$ but regard $\bar{\alpha}$ large, the viscous term (9b) becomes negligible in the x-momentum equation, while the pressure gradient (9f) still dominates the y-momentum equation. Hence for large $\bar{\alpha}$, the reattachment process is inviscid, confirming Chapman's[8] early ideas.

It is also instructive to consider $\alpha \sim R^{-n}$ with $n \leq 1/4$. The results are as follows: (i) for $n = 1/4$, the reattachment process is viscous; (ii) for $0 < n < 1/4$ but not of order one, the reattachment process is inviscid and the pressure gradient $\partial p/\partial y$ transverse to the wall vanishes; (iii) for $n = 0$ ($\alpha \sim 1$), the reattachment process is inviscid and $\partial p/\partial y$ is important.

For case (i) the complete separated flow region is contained within the triple-deck and a well-developed plateau appears only in the limit $\alpha R^{1/4} \to \infty$, which overlaps case (ii). Case (iii) includes case (ii) and was treated earlier by Burggraf.[3] Numerical results for this case were presented based on Chapman's similarity solution for the free shear layer entering the reattachment zone, corresponding to a long plateau between separation and reattachment. For a short plateau, the appropriate profile is that of Neiland given above, corresponding to case (ii).

We now formulate a calculation procedure for the reattachment zone following a short plateau. For convenience, we assume $\alpha \sim R^{-1/4}$, but regard $\bar{\alpha}$ as large so that case (ii) applies. We introduce new variables for the reattachment zone, indicated by a tilde, as $\tilde{X}$. The initial conditions entering the reattachment zone are provided by Eq. (6), and these together with the scaling of Eq. (8) imply the following relationships between new and old variables:

$$\tilde{U} = U\bar{L}_p^{-1/3} \quad , \quad \tilde{Z} = Z\bar{L}_p^{-1/3} \quad , \quad \tilde{X} = (X - X_R)\bar{L}_p^{1/3} \tag{11}$$

Here $\bar{L}_p$ is the nondimensional form of L_p, scaled as in Eq. (1), and X_R is an arbitrary origin within the reattachment zone, selected below. In addition, the stream function and vorticity are defined as

$$\tilde{\Psi} = \int_{Z_d}^{\tilde{Z}} \tilde{U} d\tilde{Z} \quad , \quad \tilde{\Omega} = \frac{\partial \tilde{U}}{\partial \tilde{Z}} \tag{12}$$

The subscript d refers to the dividing streamline; i.e., that which ultimately reattaches to the wall. Far upstream on the $\tilde{X}$ scale, $\tilde{\Omega}$ is given by Neiland's shear layer as $f_0''(\tilde{Z} - \tilde{Z}_d)$.

With these definitions, the principles of conservation of vorticity and total pressure yield

$$\tilde{U}^2 = 2\int_{\tilde{Y}_m}^{\tilde{Y}} \tilde{\rho}\,d\tilde{Y} \quad , \quad \tilde{P} = \frac{1}{2}\left(\tilde{U}_d^2 - \tilde{U}^2\right) \tag{13}$$

where $\tilde{Y}_m$ is the minimum value for $\tilde{Y}$ at the local $\tilde{X}$ station. Since $\alpha \sim R^{-1/4}$, the outer matching condition (5) applies, and the $\tilde{X}$ location is determined from the pressure:

$$\tilde{X} = \int \frac{d\tilde{A}}{\tilde{P}_f - \tilde{P}} \tag{14}$$

The origin of $\tilde{X}$ is obtained by extrapolating the dividing streamline of the free shear layer linearly to the wall, thus defining X_R above.

Equation (14) defines a unique relation for the pressure distribution in the reattachment zone. This relation is shown by the curve in Fig. 5. The plotted points shown for comparison are experimental data for a 10° compression ramp taken from Fig. 20a of Ref. 2. Since the experimental reattachment point was not defined, it was arbitrarily chosen to match the theoretical pressure at $\bar{X} = 0$. The comparison shown is reasonably good, and might be improved by accounting for the evolution of the shear layer-velocity profile over the finite plateau length.

Now consider the case of a long plateau. According to Eq. (8), L_p of order one corresponds to α of order one, and thence L_R of order $R^{-1/2}$. More explicitly, the scaling of Eq. (11) for the short plateau suggests that when $L_p \sim 1$, the physical length scale in the reattachment zone is

$$x - x_R = x_0(L_p/x_0)^{-1/3}C^{1/2}\lambda^{-5/3}(M_*^2-1)^{-1/2}(T_w/T_\infty)^2R_*^{-1/2}\tilde{X} \tag{15}$$

where Eqs. (1) and (2) have been invoked. The appearance of the λ and x_0 factors indicate the history of the upstream Blasius boundary layer; these would be expected to disappear for a truly long plateau. The Mach number and Reynolds number scaling here are exactly those deduced in Ref. 9 on the basis of physical arguments. The curves shown in Fig. 6, reproduced from Ref. 9, were calculated for inviscid reattachment of a Chapman shear layer (Ref. 11), corresponding to a long plateau with vanishingly short upstream boundary layer. Even though plotted in the Mach number scaling of Eq. (15), a residual Mach number dependence is evident. One reason is that Eq. (15) is based on Neiland's shear layer in which the velocity is small and the flow is essentially incompressible. For the long plateau with Chapman's shear layer, the flow is compressible. In addition, the flow turning angle in the latter case is large enough for nonlinear effects to be important in the pressure-angle flow relation.

Also shown in Fig. 6 are experimental data for a 25° compression ramp taken from Fig. 14a of Ref. 8. In this case, the origin was estimated by extrapolating the free shear layer visible in the schlieren photograph, an uncertain procedure. If an origin shift is allowed the comparison with theory is not bad. In general, the effect of the upstream boundary-layer history on the shear layer initiating the reattachment zone should be accounted for. This may be accomplished by calculating the shear layer as it develops downstream from Neiland's profile over the length of the pressure plateau, as demonstrated by Denison and Baum.[10]

4. GEOMETRY OF THE SEPARATED FLOW REGION

According to Neiland's[1] asymptotic structure for the separation region, the plateau region exhibits only small fluid motion, except for the free shear layer which may be calculated independently. The length of this region can be estimated from Chapman's[11] hypothesis of the reattachment pressure rise: the total pressure on the dividing streamline entering the reattachment zone equals the final pressure recovered when the external flow has been turned parallel to the wall. Using the velocity and thickness scalings given by Neiland's asymptotic shear layer as an estimate for conditions entering the reattachment zone, we have shown already that Chapman's hypothesis implies the length of the free shear layer in the plateau region to be of order $\alpha^{3/2}$. More explicitly, utilizing the linear pressure-angle relation for the external flow and Chapman's hypothesis, we have on the dividing streamline

$$P + U^2/2 = \bar{\alpha}$$

For the short plateau, the left side can be evaluated from Eq. (6). Truncating the series at the first order term in X (which we now interpret as the plateau length $\bar{L}_p$) we find

$$\bar{L}_p \sim (2[\bar{\alpha} - P_0 - f_0'(0)f_2'(0)]/[f_0'(0)]^2)^{3/2} \tag{16a}$$

Substituting the numerical values given earlier yields

$$\bar{L}_p \sim 3.47(\bar{\alpha} - 1.55)^{3/2} \tag{16b}$$

Since this is an asymptotic formula, it is valid only for $\bar{\alpha} \gg 1.55$. While we have no numerical solutions of the type shown in Fig. 1 for such large $\bar{\alpha}$, it is possible to compare with experimental data for at least one of the cases in Ref. 8, the 25° ramp. Converting the ramp angle to the nondimensional form gives $\bar{\alpha} = 6.89$ for that case. According to the above formula, $\bar{L}_p = 42.7$, while an approximate value of about 47 is found by measuring the length of the free shear on the photograph (Fig. 14a of Ref. 8). This agreement lends credence that the above asymptotic formula is useful for practical application, although additional comparison with experiment is essential.

The complete geometry of the separated region is now available. From Williams' solution,[7] the plateau shear layer is inclined at an angle α relative to the wall:

$$\bar{\alpha} - P_0 = 1.800$$

Hence from Fig. 2 and the law of sines, the distance between the ramp leading edge and the separation point is

$$X_c - X_s = \left(1 - \frac{1.8}{\bar{\alpha}}\right)\bar{L}_p \tag{17}$$

A complete pressure distribution for a 10° ramp has been calculated from the above theory and is shown in Fig. 7. The conditions correspond to those of Fig. 20a of Ref. 2, already referenced in Fig. 5. In making these calculations, it was necessary to account for an inconsistency between Eqs. (16) and the reattachment calculation outlined in Eqs. (11) through (14). Equation (16) is based on two terms of the asymptotic expansion for Neiland's shear layer, whereas the reattachment solution shown in Fig. 5 was based on only the leading term. The analysis was made consistent by dropping the term $f_2'(0)$ in (16a), or equivalently, replacing the value 1.55 in (16b) by $P_0 = 1.80$, and requiring the final pressure at the end of the reattachment zone to agree with the inviscid wedge pressure. The agreement with the experimental data in Fig. 7 is fairly good, and could be improved if the freedom of the origin shift in the asymptotic formulas is exploited to shift the theoretical reattachment zone a short distance downstream.

To compare the accuracy available with integral methods, Fig. 8 is taken from Fig. 21 of Nielsen, et al.[2] In their method, the interaction is started at a particular point which is usually chosen to make the resulting solution agree well with experiment. In Fig. 8 the four integral curves correspond to initial points of 0.0525 to 0.0700 feet from the leading edge. If the experimental data were not available, there would be no reason to prefer any of the four integral curves. Comparing Figs. 7 and 8, we conclude that the accuracy of the asymptotic theory is of the same order as that of the integral method.

5. CONCLUSIONS

The evidence presented above supports the view that the asymptotic theory of laminar separation and reattachment is an acceptable formulation for practical purposes. By combining the results of the structure of the three regions (separation, plateau, and reattachment) the complete structure of the flow field can be predicted independent of experimental inputs, although there is some room for adjustment in the theory through optimum choice of reference conditions and origin shifts in the asymptotic expansions. Further development of the Stewartson-Williams free-interaction theory is underway, with promising results both from higher-order analyses and from inclusion of hypersonic effects. Similar improvements in the reattachment theory are also necessary. Nevertheless, even in its present state, the theory can serve as a useful tool for engineering analysis.

6. REFERENCES

1. Lees, L., and Reeves, B., AIAA J. 2, 1907-1920(1964).
2. Nielsen, J., Lynes, L., and Goodwin, F., USAF FDL TR-65-107 (1965).
3. Messiter, A., Hough, G., and Feo, A., J. Fluid Mech. 60, 605-624 (1973).
4. Neiland, V., Izv. Akad. Nauk SSSR No. 3, 19-24 (1971).
5. Stewartson K., and Williams, P., Proc. Roy. Soc. A. 312, 181-206 (1969).
6. Jenson, R., Burggraf, O., and Rizzetta, D., Paper presented at 4th Int. Conf. on Numerical Methods in Fluid Mechanics, held at Boulder Colo., June 1974. To be published in conference proceedings, Springer-Verlag (1974).
7. Stewartson, K., and Williams, P., Mathematika 20, 98-108 (1973).
8. Chapman, D., Kuehn, D., and Larsen, H., NACA Rpt. No. 1356 (1958).
9. Burggraf, O., Proc. 3rd Int. Conf. on Numerical Methods in Fluid Mech., Lecture Notes in Physics, Vol. 18, Springer-Verlag (1973).
10. Denison, M., and Baum, E., AIAA J. 1, 342 (1963).
11. Chapman, D., NACA TN 3792 (1956).

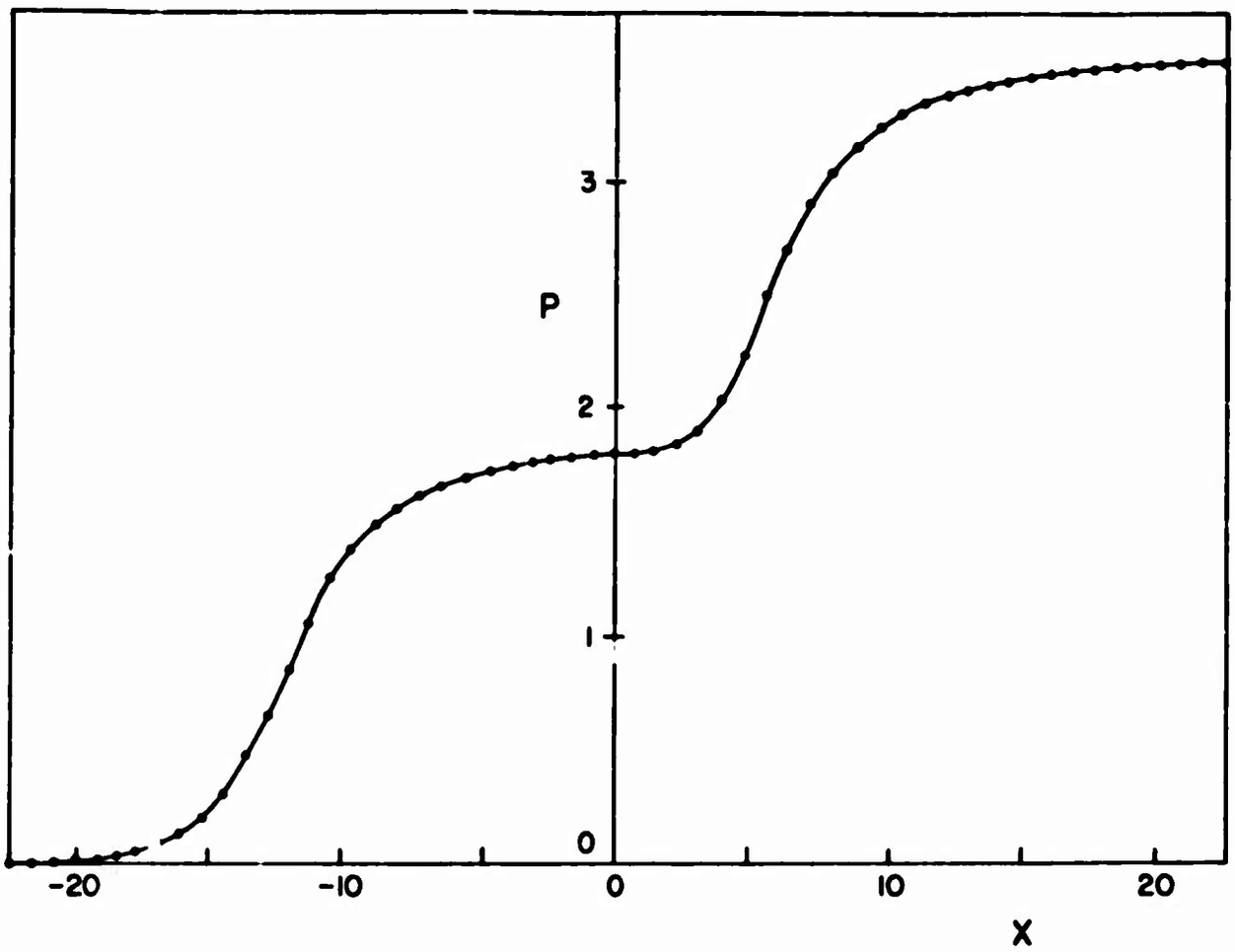

Figure 1. Wall pressure distribution for $\bar{\alpha}$ = 3.5, plotted in inner layer variables. Mesh size: ΔX = 0.8, ΔY = 0.8.

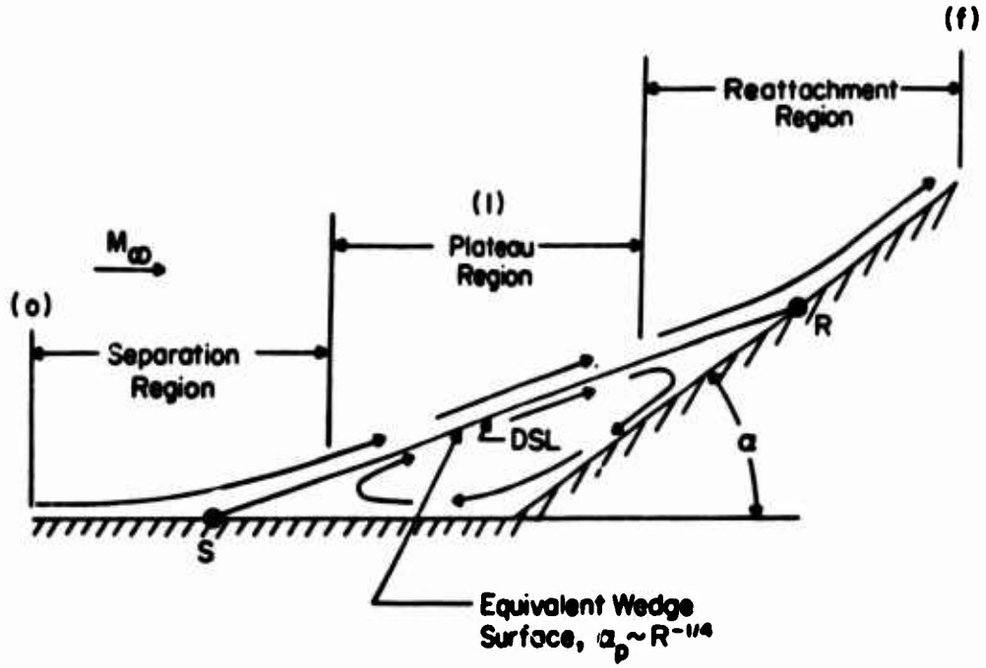

Figure 2. Geometry of the separated flow for α = O(1).

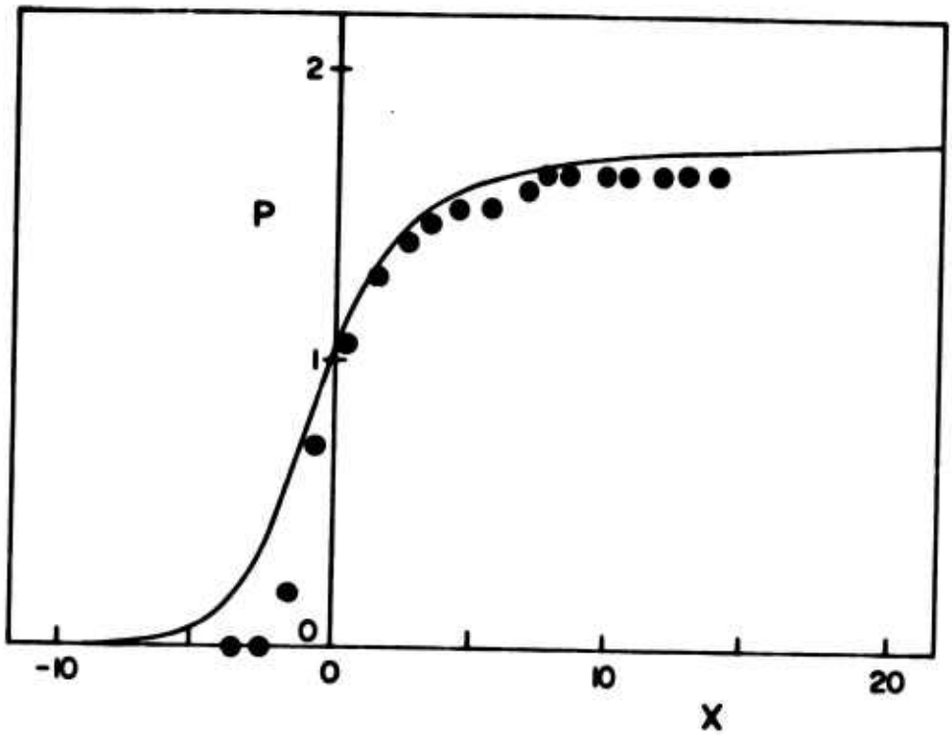

Figure 3. Pressure distribution in separation region for a forward-facing step; $M_e = M_s = 2.21$, $R_e = u_\infty x_s/\nu_\infty = 92{,}000$, $T_w/T_\infty = 1.90$. Asymptotic Theory: ———; experimental data from Ref. 8, Fig. 11a: ●.

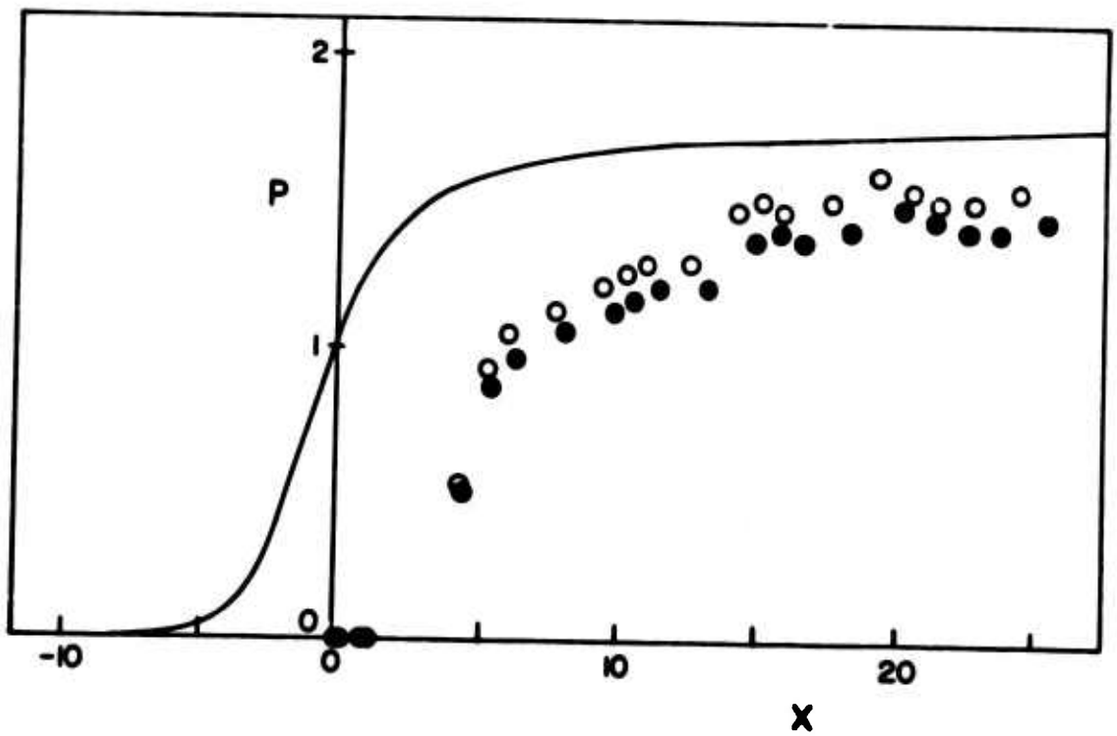

Figure 4. Pressure distribution in separation region for a curved ramp. Asymptotic theory: ———. Experimental data from Ref. 8, Fig. 17a: $M_e = M_0 = 2.7$, ●; $M_s = M_3 = 2.56$, ○. $R_e = u_\infty x_s/\nu_\infty = 39{,}000$ and $T_w/T_\infty = 2.4$ for both cases.

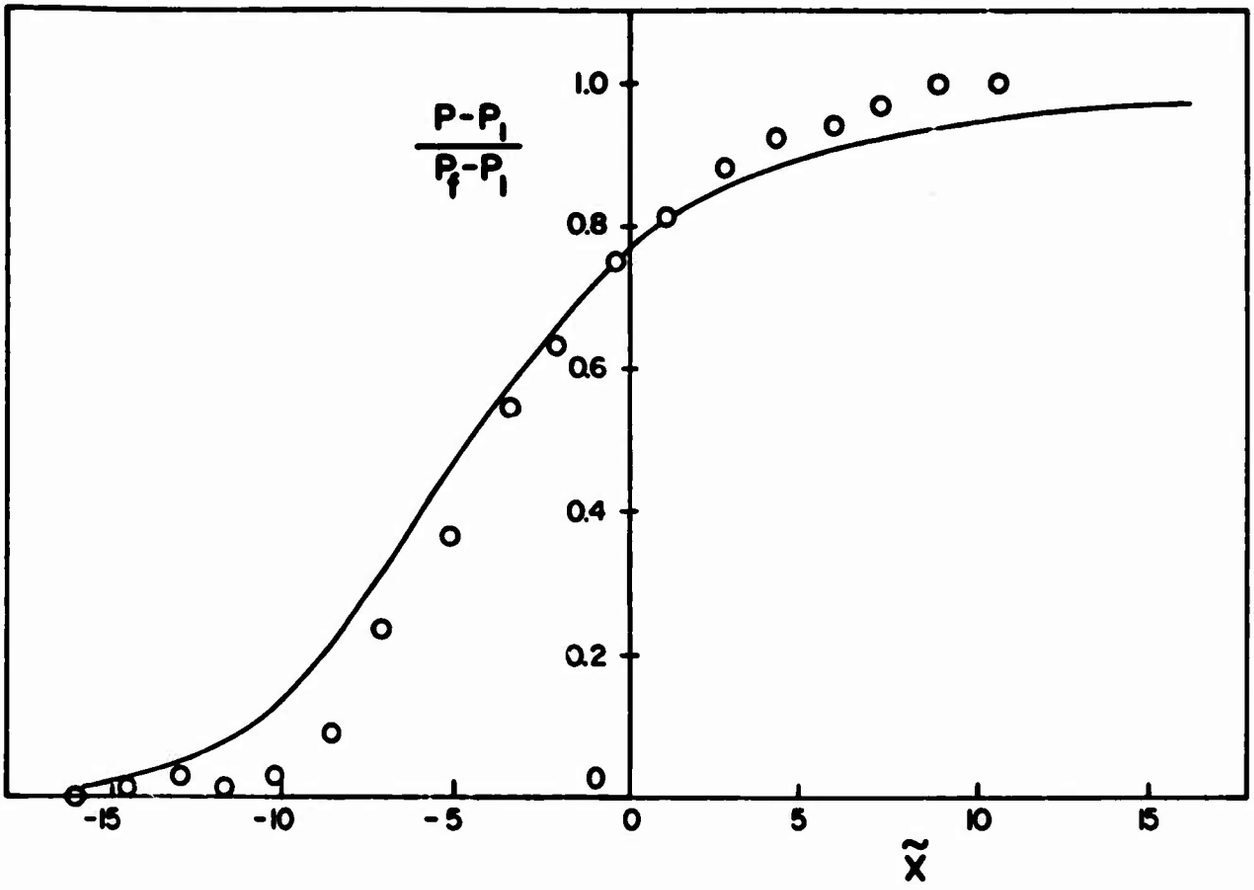

Figure 5. Pressure distribution in reattachment region with a short plateau. Theory: ——— ; experimental data from Ref. 2, Fig. 20a: O , $\alpha = 10^{\circ}$, $M_\infty = 2.55$, $R_\infty = 206{,}000$, $T_w/T_\infty = 2.11$.

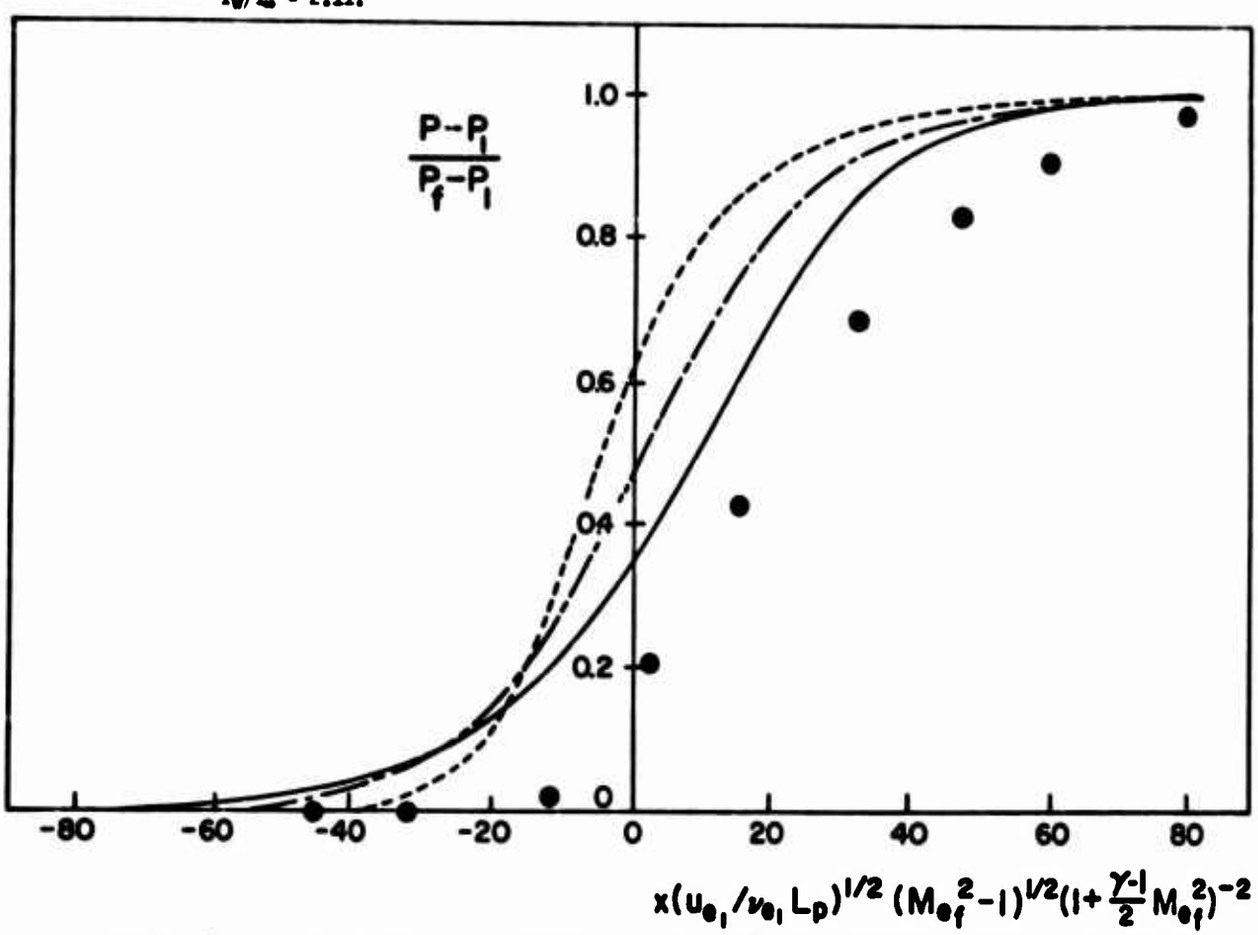

Figure 6. Pressure distribution in reattachment region with a long plateau. Theory from Ref. 9: ----, $M_{e_1} = 1.4$; — — —, $M_{e_1} = 3$; ———, $M_{e_1} = 7$. Experimental data from Ref. 8, Fig. 14a: ● , $\alpha = 25^{\circ}$, $M_\infty = 2.7$, $R_\infty = 33{,}000$, $T_w/T_\infty = 2.24$.

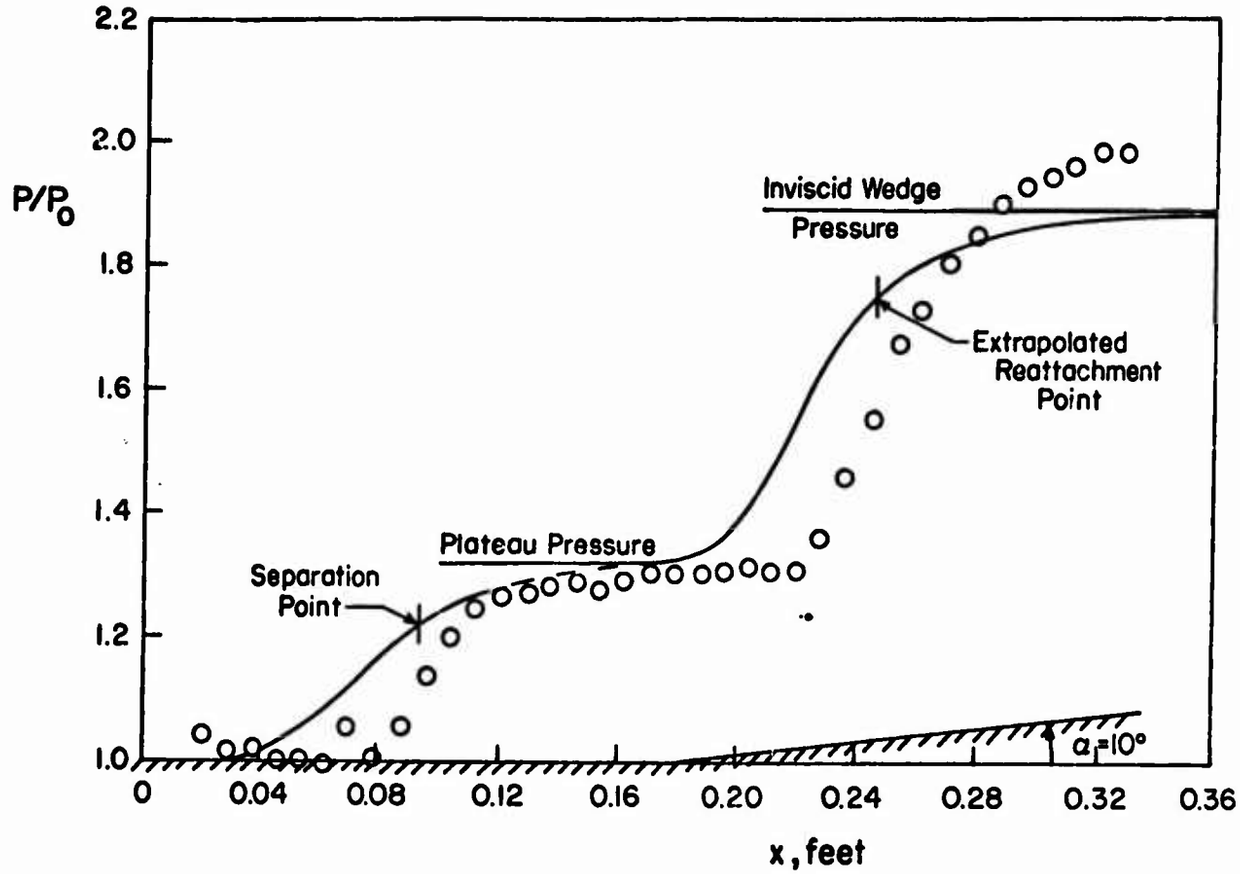

Figure 7. Overall pressure distribution for 10° ramp. Theory: _____ ; experimental data from Ref. 2, Fig. 20a: O , M_o = 2.55, R/ℓ = 1.143 x 10^6/ft.

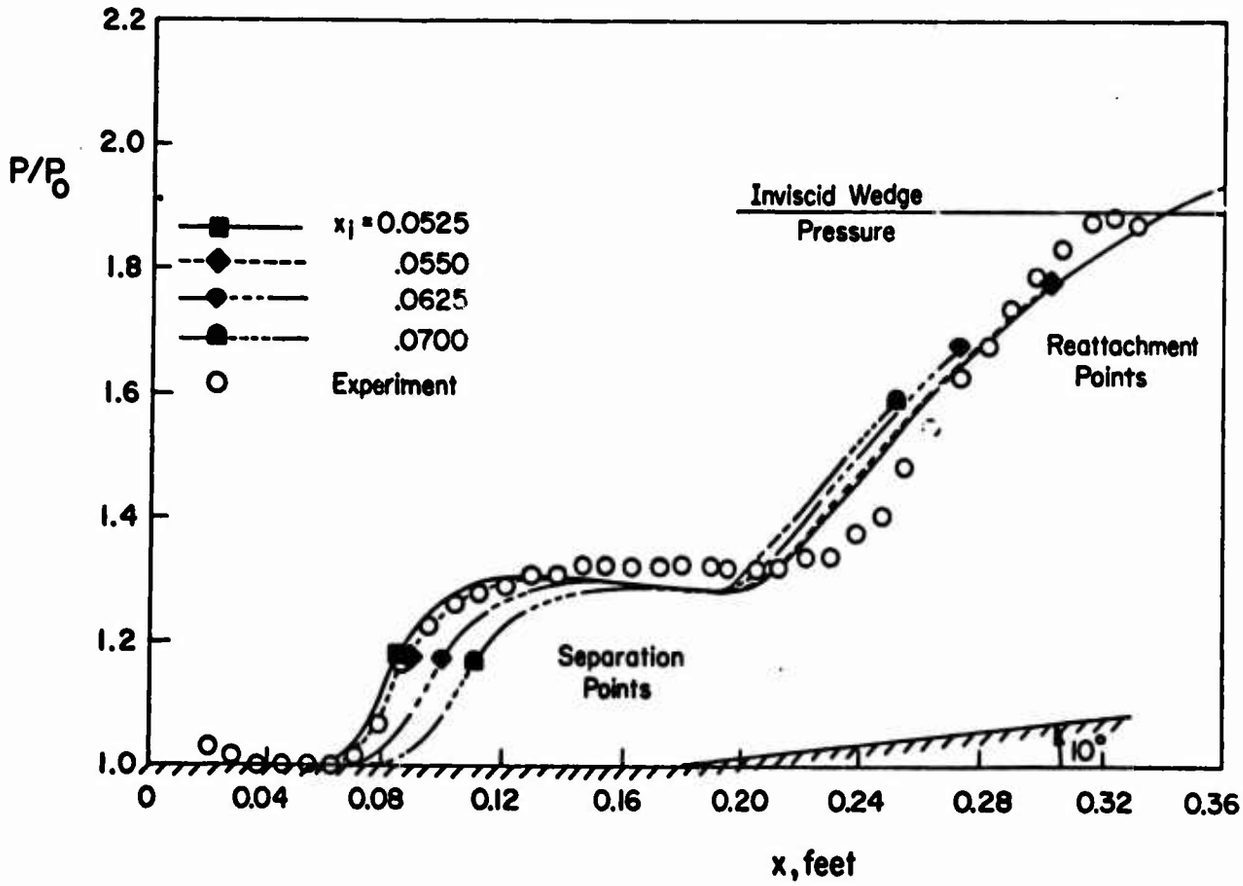

Figure 8. Nielsen integral theory - effect on calculated pressure distribution of variation in beginning of interaction x_1. Theory and experimental data from Ref. 2, Fig. 21: M_o = 2.55, R/ℓ = 85,000/ft.